

Multiscale Approximation as a Bias-Reducing Strategy for Scalar and Manifold-Valued Functions

Asaf Abas¹ and Nir Sharon¹

¹Department of Applied Mathematics, Tel Aviv University, Tel Aviv-Yafo, Israel

July 10, 2025

Abstract

We study the bias–variance tradeoff within a multiscale approximation framework. Our approach utilizes a given quasi-approximation operator, repeatedly applied in an error-correction scheme over a hierarchical data structure. We introduce a new bias measurement, the bias ratio, to quantitatively assess the improvements made by multiscale approximations and demonstrate that this multiscale strategy effectively reduces the bias component of the approximation error, thereby providing a more flexible and robust framework for addressing scattered data approximation problems. Our findings exhibit consistent bias decay across various scenarios, including applications to manifold-valued functions.

1 Introduction

Quasi-approximation is a standard approach for the smooth approximation of functions given as samples over scattered data sites [1, 2]. This type of operator has been generalized for various domains, particularly for functions defined on manifolds, e.g., [3, 4, 5, 6]. Quasi-approximation is recognized for its ability to reproduce specific function spaces, preserving stability and locality, while maintaining low computational complexity. However, the smooth results it outputs often lead to high-bias approximations.

To enhance the above qualities, we propose a strategy to address high-bias approximation. Specifically, we investigate the application of quasi-approximation in a multilevel scheme. This strategy utilizes nested sets from the data and applies error correction across different scales, enabling a more effective capture of finer details. Initially proposed in the context of radial basis functions [7], this hierarchical error correction scheme can be easily extended to many types of approximation operators.

Recent studies on multiscale have focused on analyzing the error rates associated with the multiscale approach [8, 9], while others have adapted it to new settings [6] or made improvements [10]. A line of research has expanded the Nyström extension with multiscale error correction schemes [11, 12]. This approach has applications in dimension reduction using diffusion maps [13, 14]. In contrast to our settings, the Nyström extensions exclusively utilize the Gaussian kernel.

This paper investigates how the multiscale method can reduce the bias term in quasi-approximation. We begin by reviewing a necessary background, including our definitions and the bias-variance tradeoff. In this context, the bias-variance tradeoff is often used as a tuning guideline for approximation [15, 16], and has also served as a tool for statistical analysis [17, 18]. Here, we propose a new measure that describes the bias-variance tradeoff, the bias ratio, and examine its behavior through numerical experiments across diverse settings. Our results show that increasing the number of multiscale levels consistently reduces the bias, suggesting that this approach can serve as an effective approximation mechanism in practical applications.

2 The multiscale approximation and the bias-variance tradeoff

We start with the basic definitions and notation. Let $f: \mathbb{R}^d \rightarrow \mathcal{M}$ be our target function to approximate. Here, d and \mathcal{M} are given. \mathcal{M} is a Hadamard manifold, also known as Cartan–Hadamard manifolds, which are simply connected, complete, and have non-positive sectional curvature. For Hadamard manifolds, the geodesic distance $\rho: \mathcal{M} \times \mathcal{M} \rightarrow \mathbb{R}$ exists and is unique for any pair of two points in \mathcal{M} [19].

In this paper, we focus on approximating scattered data. Specifically, the data consists of the set of tuples $X = \{(x_i, f_i)\}_{i=1}^N$ where $\{x_i\}_{i=1}^N \subseteq \mathbb{R}^d$ are the parametric data sites, and $\{f_i\}_{i=1}^N \subseteq \mathcal{M}$ are the observable samples. The data sites are not limited to a grid-like formation or by any other restriction. Noise may contaminate these observations, modeled as $f_i = f(x_i) + \nu_i$, where ν_i is the noise term. The goal is to approximate the value of the function $f(x^*)$, for a new data site $x^* \in \mathbb{R}^d$.

This section details the multiscale framework for scalar-valued and Hadamard manifold-valued functions. Additionally, we present the bias-variance tradeoff and propose a new measurement based on it, the bias ratio.

2.1 The multiscale approximation

The multiscale approximation, also known as multilevel approximation, serves as an error correction scheme for improving approximation, which was first introduced in [7]. This method can enhance the results of a given operator without any additional data or assumptions [6, 8, 9, 10, 11, 14]. The multiscale approximation is based upon two main procedures: generating a sequence of nested hierarchical sets and applying a given operator Q through error correction schemes.

A hierarchical sequence of subsets of X satisfies $X_1 \subset \dots \subset X_n = X$. Each subset X_i corresponds to a scale (or level) of the multiscale. The number of scales n is a parameter. Throughout this work, we generate the subsets randomly. Their size satisfies a given proportional growth rate $\lambda \sim \#X_{i-1}/\#X_i$. Additionally, the multiscale scheme involves deploying a given “black-box” approximation operator Q . We focus on quasi-interpolation operators. We denote the approximation of Q over the dataset X_j with the target function f by $Q_j f = Q_{X_j} f$.

The error correction scheme defines a sequence of operators $\{M_i\}_{i=1}^n$, each associated with a corresponding subset $\{X_i\}_{i=1}^n$. The literature presents two equivalent approaches for expressing the multiscale operators M_i : an iterative approach [7] and a direct approach [9]. While the direct approach is commonly used for theoretical analysis, the iterative approach offers practical advantages for numerical implementation. The iterative approach constructs two sequences of operators: the multiscale

approximation operators $\{M_i\}_{i=1}^n$ and the multiscale error operators $\{E_i\}_{i=1}^n$. The initial conditions are $M_0 = 0$ and $E_0 f = f$. At each step i , the method updates the operators according to:

$$\begin{aligned} M_i f &= M_{i-1} f + Q_i E_{i-1} f, \\ E_i f &= E_{i-1} f - Q_i E_{i-1} f. \end{aligned} \tag{1}$$

After completing n steps, this process produces the approximated function $\tilde{f} = M_n f$.

The numerical implementation of the multiscale for scalar-valued functions is straightforward (1). In [6], the authors discuss the generalizations that are needed to approximate a manifold-valued function, and we incorporate their modifications in our work. The modifications include switching the plus and minus operations to the exponential map and logarithmic map, respectively.

2.2 Bias-Variance Tradeoff for scalar and manifold-valued functions

The bias-variance tradeoff (BVT) is extensively studied and applied across various fields, such as statistics, signal processing, and more. Notable applications of the BVT include statistical analysis [17, 18] and algorithm tuning [15, 16]. This section introduces the BVT in the context of approximating scalar-valued functions and Hadamard manifold-valued functions.

Let \tilde{f} be an approximation of a scalar-valued target function $f: \mathbb{R}^d \rightarrow \mathbb{R}$. The mean squared error (MSE) of \tilde{f} is

$$\text{MSE}[\tilde{f}, f](x) = \mathbb{E} \left[(f(x) - \tilde{f}(x))^2 \right], \tag{2}$$

where $\mathbb{E}[\cdot]$ denotes the expected value with respect to the sampling of the domain and the noise. The BVT decomposes the MSE into two components: bias and variance. The decomposition is expressed as

$$\text{MSE}[\tilde{f}, f](x) = \text{Bias}^2[\tilde{f}, f](x) + \text{Var}[\tilde{f}](x),$$

where

$$\begin{aligned} \text{Bias}^2[\tilde{f}, f](x) &= \left(\mathbb{E} \left[f(x) - \tilde{f}(x) \right] \right)^2, \\ \text{Var}[\tilde{f}](x) &= \mathbb{E} \left[\left(\tilde{f}(x) - \mathbb{E}[\tilde{f}(x)] \right)^2 \right]. \end{aligned} \tag{3}$$

As in most scenarios, we are unable to compute these terms directly and can only approximate them. To this end, we perform several trials. From N different trials, we compute a set of approximations $\{\tilde{f}^1, \dots, \tilde{f}^N\}$. We use their average as an estimation for the expected value,

$$\mathbb{E} \left[\tilde{f}(x) \right] \approx \frac{1}{N} \sum_{j=1}^N \tilde{f}^j(x). \tag{4}$$

Next, we revise the above definitions for the case of a manifold-valued function, $F: \mathbb{R}^d \rightarrow \mathcal{M}$. The extension of (2) and (3) is achieved using the geodesic distance ρ associated with the Hadamard manifold \mathcal{M} . In particular, it is a common technique

in calculating the MSE over a manifold to measure the error using the geodesic distance squared, e.g., [20]. Therefore, we define the MSE of an approximation \tilde{F} of the manifold-valued target function F as

$$\text{MSE}[\tilde{F}, F](x) = \mathbb{E} \left[\rho(F(x), \tilde{F}(x))^2 \right]. \quad (5)$$

For completeness, we present the remaining definitions:

$$\text{Bias}^2[\tilde{F}, F](x) = \rho \left(\mathbb{E}_{\mathcal{M}}[\tilde{F}(x)], \mathbb{E}_{\mathcal{M}}[F(x)] \right)^2, \quad (6)$$

$$\text{Var}[\tilde{F}](x) = \mathbb{E} \left[\rho \left(\mathbb{E}_{\mathcal{M}}[\tilde{F}(x)], \tilde{F}(x) \right)^2 \right]. \quad (7)$$

In order to extend (4) into manifold-valued functions, we introduce $\mathbb{E}_{\mathcal{M}}$ as the expected value in the manifold \mathcal{M} . We use the Karcher mean as a numerical approximation of the expected mean. In Hadamard manifolds, the Karcher mean exists and is unique, for nonnegative weights [21].

2.3 Measurement: The Bias Ratio

We focus on the effect of multiscale approximation on the bias component in the MSE. To enable comparison of the bias across different approximation operators without being affected by their varying MSE values, we suggest the bias ratio:

$$\text{Br}[\tilde{f}, f](x) = \frac{\text{Bias}^2[\tilde{f}, f](x)}{\text{MSE}[\tilde{f}, f](x)}. \quad (8)$$

As a relative measure, the bias ratio is expressed as a percentage.

3 Numerical Evaluation

We numerically demonstrate the effect of the multiscale on the bias ratio (8). The demonstrations include a series of numerical experiments that test the multiscale in various approximation methods, target functions, and noise levels.

We open the numerical experiments section by applying the multiscale method to a moving least squares approximation. Our target function is a smooth, scalar-valued function, and we conduct experiments with various dataset sizes. We demonstrate how the multiscale method achieves a significantly lower bias ratio and a superior error rate. These findings may indicate the potential of the multiscale to address a suboptimal choice of hyperparameters. Next, we switch to Shepard approximation [22]. We compare the Shepard approximation and its multiscale version for a noisy, high-bias, scalar-valued target function. Specifically, we investigate the multiscale behavior as a function of the SNR. In the final experiment, we change the setting to a manifold-valued function, i.e., we choose the manifold of symmetric positive definite (SPD) matrices.

3.1 Settings of the Numerical Framework

Next, we outline the settings of the numerical experiments. We use a scattered dataset X , which is sampled uniformly from $[0, 1]^2$. The hierarchical sequence of nested subsets is determined by three parameters: 1) the dataset X , 2) the number

of layers, and 3) the proportional growth rate λ . The growth rate λ controls the size of each subset in the hierarchical sequence; we set $\lambda = 80\%$. All the results are for a three-layer multiscale. In our experiments, we found that the marginal contribution was low for more than three layers. In each layer, the data points are randomly sampled from X . For each data point in the graphs, we repeat the process of generating datasets, hierarchical sequences, and sample noise, and apply approximations for 100 trials.

In the results sections, we track two key metrics: the MSE (2) and the bias ratio (8). We inspect these metrics through their 25th, 50th, and 75th percentiles. In each experiment, we compare a chosen approximation scheme (referred to as “singlescale”) and its multiscale counterpart. The code is publicly available¹.

3.2 Multiscale based on linear moving least squares over scattered data

We examine the multiscale for moving least squares approximation (MLS). Our MLS implementation is based on inverting the system of equations, and we limit the MLS to polynomials up to degree 1. We select a Gaussian for the radial kernel function $K(r) = e^{-2(r/\delta)^2}$, where δ represents three times the mesh norm of the dataset.

In this experiment, we compare the MLS and its multiscale behaviors over a smooth, scalar-valued target function,

$$f(x, y) = e^{x^2+y^2} + 3, \quad (9)$$

without incorporating a noise term. We investigate the multiscale behavior over various dataset sizes.

Figure 1 reveals several key observations. Notably, the plain MLS exhibits a high bias, approaching 100%, suggesting it may be a suboptimal choice in this context. In contrast, its multiscale achieves a significantly lower bias ratio. Additionally, Figure 1b shows that the multiscale method yields substantially lower error rates, supporting the hypothesis that it captures data patterns more effectively. This also indicates that the multiscale approach is more robust to suboptimal hyperparameter choices, such as the selection of the kernel function.

3.3 Multiscale based on Shepard approximation with noisy data

Following [6], we compare the traditional Shepard approximation [22] with its multiscale version. Given a dataset $X = \{(x_i, f_i)\}_{i=1}^N$, the Shepard approximation at a point s is computed as follows: $\sum_{i=1}^N f_i K(r_i) / \sum_{i=1}^N K(r_i)$, where $r_i = \delta^{-1} \|x_i - s\|_2$ and δ is defined as in Section 3.2. We use the radial kernel $K(r) = (\max\{1 - r, 0\})^4 \cdot (4r + 1)$ from [1].

We analyze the performances over the target function (10), which has a grid-like wave pattern. This pattern generates high local bias. The function is

$$f(x, y) = \sin(2\pi x) \cos(4\pi y) (1 + \nu \cdot p). \quad (10)$$

Here, the noise term ν is sampled from $\mathcal{N}(0, 1)$ at every evaluation of the target function, and the constant p acts as the standard deviation of the Gaussian noise. In each trial, we sample approximately 14^2 uniformly random points from $[0, 1]^2$.

¹https://github.com/ABASASA/Multiscale_Bias_Ratio

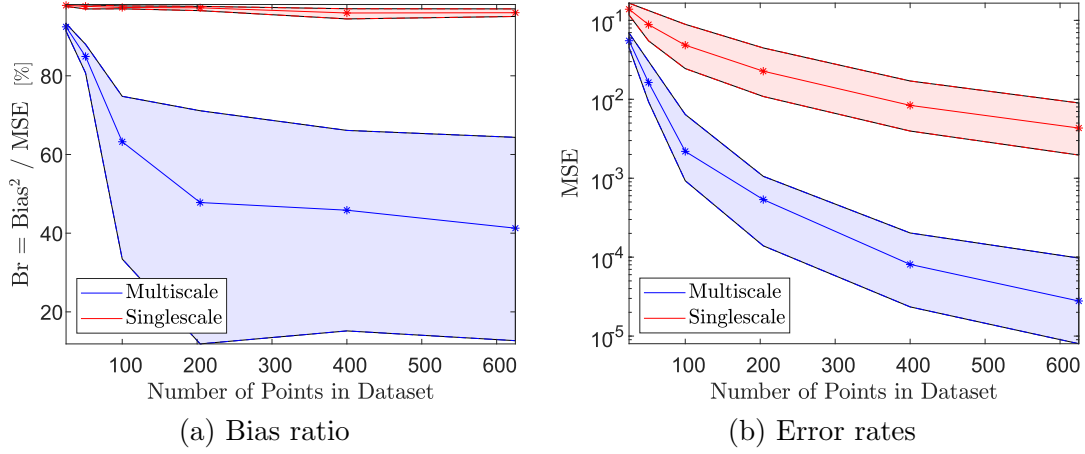


Figure 1: Comparing MLS (red) and its multiscale (blue) across different sizes of datasets. The target function is a smooth scalar-valued function (9).

Figure 2 illustrates the comparison of Shepard (singlescale) and its multiscale for different signal-to-noise ratios (SNR), $\text{SNR} = 1/p^2$. Figure 2a demonstrates a lower bias ratio for the multiscale for any SNR. In addition, Figure 2b supports several past works, the multiscale suggests a preferable error rate. Specifically, the multiscale results in lower error rates, as indicated by the median and tighter 25th and 75th percentiles, for $\text{SNR} > 0.5$. However, for sufficiently high noise levels, both methods exhibit similar error rates. The similar error rates suggest Shepard performs well, leaving little room for multiscale improvement.

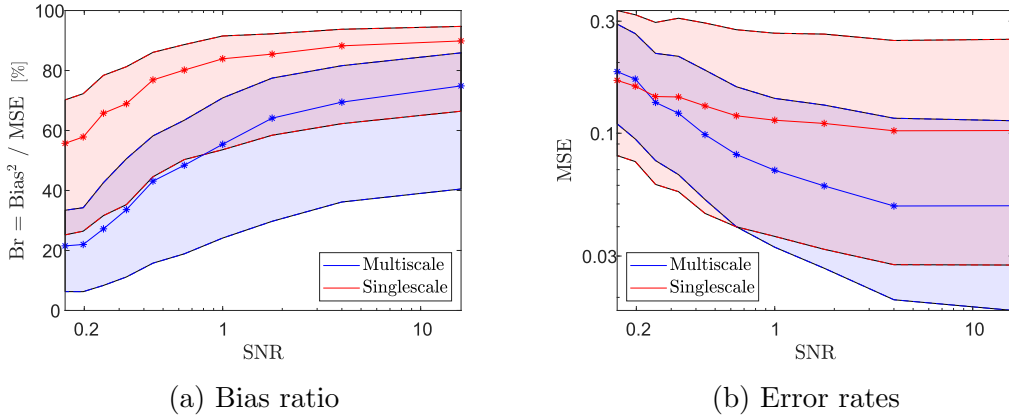


Figure 2: Comparing Shepard (red) and its multiscale (blue) across different noise-to-signal ratios. The target is a noisy scalar-valued function with a pattern that generates high local bias (10).

3.4 Approximating function with values on a Hadamard manifold

We extend our previous experiment into a symmetric positive definite (SPD) manifold setting, which is a special case of a Hadamard manifold. We define the multiscale operators over the manifold according to [6]. The target function and the noise are defined in the tangent space, symmetric matrices, and projected to the SPD manifold:

$$G(x, y) = \exp_{\mathcal{M}}(A(x, y)(I + \Sigma \cdot p)), \quad (11)$$

where $A(x, y) = \begin{pmatrix} \sin(2\pi y) \cos(2\pi x) & y^2 & xy \\ y^2 & 1 & 0 \\ xy & 0 & \cos(\pi x) \end{pmatrix}$. Here, $\exp_{\mathcal{M}}$ is the matrix exponential, Σ is a symmetric matrix whose entries are sampled independently and identically from $\mathcal{N}(0, 1)$, and p represents a predetermined noise constant. In this case, we do not have an analytical expression for the SNR. Instead, we use the numerical mean of $\text{SNR}(x, y) = \|A(x, y)\|_F^2 / \|A(x, y) \cdot \Sigma\|_F^2$ over $[0, 1]^2$ where $\|\cdot\|_F$ is the Frobenius norm. The dataset consists of approximately 11^2 points, which are sampled uniformly at random from the square $[0, 1]^2$.

Based on the version of the BVT to manifold (5)-(7), we compare the Shepard approximation and its multiscale version. As in the previous examples, in Figure 3a, the multiscale demonstrates a significantly lower bias ratio. In Figure 3b, the multiscale suggests superior error rates.

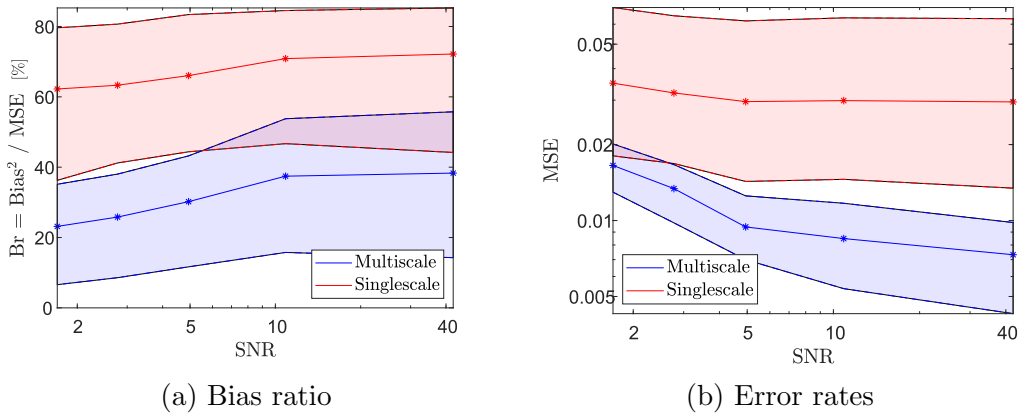


Figure 3: Comparing Shepard (red) and its multiscale (blue) across different noise-to-signal ratios. The target function is a noisy manifold-valued function (11).

4 Acknowledgements

NS is partially supported by the DFG award 514588180.

References

- [1] H. Wendland, *Scattered data approximation*, vol. 17. Cambridge university press, 2004.
- [2] D. Levin, “The approximation power of moving least-squares,” *Mathematics of computation*, vol. 67, no. 224, pp. 1517–1531, 1998.
- [3] P. Grohs, M. Sprecher, and T. Yu, “Scattered manifold-valued data approximation,” *Numerische mathematik*, vol. 135, pp. 987–1010, 2017.
- [4] P. Grohs, M. Holler, and A. Weinmann, *Handbook of variational methods for nonlinear geometric data*. Springer, 2020.
- [5] R. Zimmermann, “Manifold interpolation,” *Model Order Reduction*, vol. 1, pp. 229–274, 2021.

- [6] N. Sharon, R. S. Cohen, and H. Wendland, “On multiscale quasi-interpolation of scattered scalar-and manifold-valued functions,” *SIAM Journal on Scientific Computing*, vol. 45, no. 5, pp. A2458–A2482, 2023.
- [7] M. S. Floater and A. Iske, “Multistep scattered data interpolation using compactly supported radial basis functions,” *Journal of Computational and Applied Mathematics*, vol. 73, no. 1-2, pp. 65–78, 1996.
- [8] H. Wendland, “Multiscale analysis in Sobolev spaces on bounded domains,” *Numerische Mathematik*, vol. 116, pp. 493–517, 2010.
- [9] T. Franz and H. Wendland, “Multilevel quasi-interpolation,” *IMA Journal of Numerical Analysis*, 2022.
- [10] S. Le Borne and M. Wende, “Multilevel interpolation of scattered data using \mathcal{H} -matrices,” *Numerical Algorithms*, vol. 85, no. 4, pp. 1175–1193, 2020.
- [11] A. Bermanis, A. Averbuch, and R. R. Coifman, “Multiscale data sampling and function extension,” *Applied and Computational Harmonic Analysis*, vol. 34, no. 1, pp. 15–29, 2013.
- [12] N. Duchateau, M. De Craene, M. Sitges, and V. Caselles, “Adaptation of multiscale function extension to inexact matching: application to the mapping of individuals to a learnt manifold,” in *International Conference on Geometric Science of Information*, pp. 578–586, Springer, 2013.
- [13] N. Rabin and R. R. Coifman, “Heterogeneous datasets representation and learning using diffusion maps and laplacian pyramids,” in *Proceedings of the 2012 SIAM International Conference on Data Mining*, pp. 189–199, SIAM, 2012.
- [14] E. Chiavazzo, C. W. Gear, C. J. Dsilva, N. Rabin, and I. G. Kevrekidis, “Reduced models in chemical kinetics via nonlinear data-mining,” *Processes*, vol. 2, no. 1, pp. 112–140, 2014.
- [15] S. Geman, E. Bienenstock, and R. Doursat, “Neural networks and the bias/variance dilemma,” *Neural computation*, vol. 4, no. 1, pp. 1–58, 1992.
- [16] K. Zhang, B. Khosravi, S. Vahdati, S. Faghani, F. Nugen, S. M. Rassoulinejad-Mousavi, M. Moassefi, J. M. M. Jagtap, Y. Singh, P. Rouzrokh, and B. J. Erickson, “Mitigating bias in radiology machine learning: 2. model development,” *Radiology: Artificial Intelligence*, vol. 4, no. 5, p. e220010, 2022.
- [17] Y. Kazashi and F. Nobile, “Density estimation in RKHS with application to korobov spaces in high dimensions,” *SIAM Journal on Numerical Analysis*, vol. 61, no. 2, pp. 1080–1102, 2023.
- [18] R. Kohavi and D. H. Wolpert, “Bias plus variance decomposition for zero-one loss functions,” in *ICML*, vol. 96, pp. 275–283, Citeseer, 1996.
- [19] P. Li, *Geometric analysis*, vol. 134. Cambridge University Press, 2012.
- [20] I. H. Jermyn, “Invariant Bayesian estimation on manifolds,” *The Annals of Statistics*, vol. 33, no. 2, pp. 583 – 605, 2005.

- [21] S. Hüning and J. Wallner, “Convergence of subdivision schemes on Riemannian manifolds with nonpositive sectional curvature,” *Advances in Computational Mathematics*, vol. 45, pp. 1689–1709, 2019.
- [22] D. Shepard, “A two-dimensional interpolation function for irregularly-spaced data,” in *Proceedings of the 1968 23rd ACM national conference*, pp. 517–524, 1968.